NPL Report DQL-OR 008

NPL Measurement report for the UV Scale 200 – 350 nm.

Heather M. Pegrum
Emma R. Woolliams
Nigel P. Fox
Andy D. Sibley

October 2004

NPL Measurement report for the UV Scale 200 – 350 nm.

Heather M. Pegrum, Emma R. Woolliams, Nigel P. Fox. Andy D. Sibley

October 2004

ISSN 1744-0610

National Physical Laboratory
Teddington, Middlesex, UK, TW11 0LW

Approved on behalf of the Managing Director, NPL, by N. P. Fox, authorised by Director Quality of Life Division

CONTENTS

1 Introduction

The NPL spectral irradiance scale from 250 to 2500 nm was formerly integrated into our measurement services and consequently became our disseminated scale in May 2003, as reported at the last CCPR meeting. This report describes the extension of this scale down to 200 nm and the transfer of the scale to deuterium lamps. The scale is based on the use of the absolute spectral radiance emitted from a high temperature blackbody through Planck's law. The critical input variable being thermodynamic temperature, which is determined by a filter radiometer whose spectral response has been calibrated against the NPL primary standard cryogenic radiometer. This traceability chain is shown schematically in Figure 1, [1]. A brief overview of the various components and stages involved in this process, together with their associated uncertainty follows below.

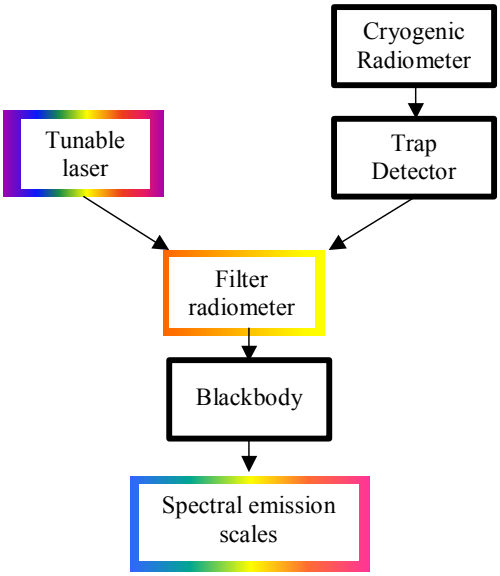

Figure 1 Traceability chain for the primary spectral irradiance scale at NPL

2 The Spectral Radiance and Irradiance Primary Scales (SRIPS) Facility

The Spectral Radiance and Irradiance Primary Scales (SRIPS) facility, shown schematically in Figure 2, was used for establishing the NPL UV spectral irradiance scale. The primary source was a BB3500 blackbody source, operated at temperatures around 3060 K and 3160 K. The thermodynamic temperature of the blackbody was determined absolutely using a group of filter radiometers built at NPL and calibrated traceably to the primary cryogenic radiometer at NPL.

A Bentham DTM300 turret grating monochromator was used to select the wavelengths and measurements were made with a photo-multiplier tube. The monochromator and detector were mounted on a large translation stage that could be moved in front of each source in turn. The entire facility was computer controlled.

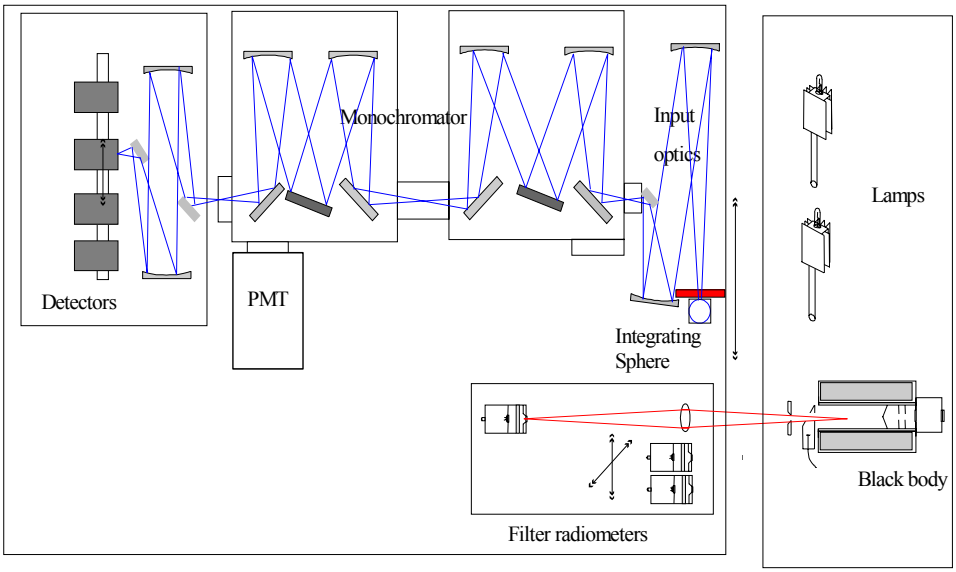

Figure 2 SRIPS Facility diagram

2.1 The Blackbody Source

The primary source was a BB3500 blackbody supplied to NPL by VNIIOFI in early 1999. The source has been extensively investigated and shown to be uniform and stable under active optical stabilisation from the front.

Investigations have shown [2] that this blackbody suffers from the same ultraviolet absorption around 380 nm as has been observed with the BB3200pg [3]. Further investigations showed that there were further absorption features at shorter wavelengths. For this reason, the blackbody temperature was kept relatively low, around 3050 K for the longer wavelengths. However, for the shortest wavelengths, a high blackbody temperature was unavoidable; here the absorption effect has been characterised and corrected.

The radiance of the blackbody was determined from Planck's law, based on a measure of its thermodynamic temperature via filter radiometers (see section 2.4), and the geometry defined by a water-cooled, brass, diamond-turned, aperture in front of the blackbody and the aperture on the integrating sphere at the front of the monochromator.

2.2 The Monochromator

The monochromator used was a Bentham DTM300 monochromator, arranged in a subtractive mode configuration. The monochromator used two UV optimised gratings. Details of the UV gratings are shown in Table 1.

Grating	Grooves per mm	Blaze Wavelength	Recommended Wavelength Range
UV	2400	250 nm	200 nm – 675 nm

Table 1 Description of the UV grating.

Light enters the monochromator via two off-axis parabolic mirrors which image the exit port of a 50 mm diameter Spectralon coated integrating sphere, onto the entrance slit of the monochromator. Both mirrors are UV enhanced, $MgFl_2$ protected, aluminium-coated mirrors. There is a 1.6 times demagnification between the integrating sphere and the entrance slit of the monochromator.

2.3 Detector

The Photomultiplier tube (PMT) is directly mounted on the exit port of the monochromator. The PMT has its own power supply and controller that stabilises it at 780V and –10 °C. For the wavelength range of these UV measurements, the PMT was the only detector used.

2.4 Filter Radiometers

The blackbody temperature was measured with an 800 nm filter radiometer used in conjunction with a geometric system to allow it to measure spectral radiance, in a similar manner to that described previously [4]. The measurement of spectral radiance with a filter radiometer gives a direct measurement of thermodynamic temperature, rather than a measurement of ITS-90 temperature obtained with a pyrometer.

The filter radiometer comprised a diamond-turned brass aperture, a wedged 10 nm bandwidth interference filter and a silicon photodiode and was housed in a water-cooled jacket. A Vinculum transimpedance amplifier was connected to the silicon photodiode and held in the same water jacket.

A 300 mm focal length lens was used at a distance of 600 mm to image light from the blackbody aperture so as to overfill the filter radiometer aperture. This aperture and a thin-film aperture on the lens defined the geometry of the measurement. The filter radiometer was used in the same f/55 geometry in which it had been calibrated. The lens transmittance was calculated using the Fresnel equations, which had previously [5] been shown to agree within 0.05 % of the measured value at this wavelength. A correction was also applied for differences in "size-of-source" based on measurements using similar techniques to those described previously [4].

Additional filter radiometers operating in "irradiance mode" (without a lens) were used to monitor any drift in the primary filter radiometer.

2.5 Instrumentation Providing Traceability

The filter radiometer used for this scale realisation was the 800 nm filter radiometer known as FR 800W50S1337A[*]. It was last calibrated in October 2002 on the filter radiometer calibration facility at NPL. It was used with a lens, the lens aperture was 10.99359 ± 0.0001 mm in diameter and was set at a distance of 600 mm ± 0.2 mm from the filter radiometer aperture (measured using measuring stick PS20131, calibrated in October 2003 It was used with the amplifier PS20171 on 10^5 gain which had been calibrated in November 2001, the calibration was reconfirmed after these measurements in June 2004.

The lamp-integrating sphere and blackbody-integrating sphere distances were set using the same measuring stick. The integrating sphere aperture was a 16 mm brass diamond turned aperture, with the serial number BJ16ED50DT[†].

The lamp electrical current was set using resistor PS5201.

Results were recorded in the following lab-books:

COAM/ORM/17/04/HMP/New SRIPS/002

COAM/ORM/17/04/HMP/SRIPS 04-07/001

[*] Note, this filter radiometer is at 800 nm with a bandwidth of approximately 20 nm and uses a Hamamatsu S1337 Si photodiode. The 'W50' in its name was an error made in the naming process and does not mean a width of 50 nm.

[†] Unique identifier BJ: 16 mm aperture "External Diameter 50", "Diamond Turned"

Electronic files are stored in:

P://QR0114/data/UV intercomparison

2.6 Laboratory Conditions

Measurements were made in a laboratory maintained at 20 ± 3 ºC. The humidity of the laboratory was not controlled.

3 Scale realisation and traceability

3.1 Overview

The traceability to SI comes from the determination of the blackbody temperature through filter radiometry. Filter radiometers were calibrated by comparison with two trap detectors against a tuneable laser-illuminated integrating sphere source. Measurements were made in approximately 0.1 nm intervals across the full transmittance range of the filter radiometer. The trap detectors, in turn, were calibrated against the cryogenic radiometer. This was done with a direct laser beam as a source. The calibrated aperture on the trap detector was used to convert spectral responsivity to spectral irradiance responsivity. A more detailed description of this process can be found in the literature [6].

3.2 Measurement Sequence

All lamps were measured on at least three occasions. The lamps were realigned between these measurements. Each calibration was made in four spectral regions, which overlapped with the neighbouring region by at least 2 wavelengths, with one exception. Regions 3 and 4 can be considered one region – a break was made simply to measure the blackbody temperature – therefore there were no wavelength overlaps between these two regions. The different regions are listed in Table 2.

Name	Start wavelength	Stop wavelength	Step size and extra wavelengths	Input optics	Slit size (mm) [Entrance – Middle – Exit]	UHTBB Temp
Region 1	200 nm	230 nm	10 nm	Tile	[3-3-5]	3160 K
Region 2	220 nm	260 nm	5 nm	Tile	[1-1-2]	3160 K
Region 3	220 nm	280 nm	10 nm + 225 nm	Sphere	[1-1-2]	3050 K
Region 4	290 nm	350 nm	10 nm	Sphere	[1-1-2]	3050 K

Table 2 Wavelengths at which the deuterium lamps were measured

Due to low signal levels between 200 and 260 nm, the integrating sphere on the SRIPS facility was replaced with a Spectralon tile diffuser. These measurements are considered only relative, as there was no defining aperture used. The results have been corrected and shifted to overlap the results from regions 3 and 4, which were made with the integrating sphere.

To further increase the signal level at the lowest wavelengths (200 – 230 nm), the entrance slits of the monochromator were widened. This introduces a further shift to the data in that region due to the bandwidth, which was corrected as described in section 4.2.1. The slit widths correspond to the

identical entrance and middle slits required by the subtractive mode monochromator, and an increased exit slit to prevent aberration losses.

For region 1 and 2 the measurements were made in the following sequence:

1) Measurement of the temperature of the blackbody with a filter radiometer.
2) Measurement of the blackbody with the SRIPS monochromator over a particular wavelength range, e.g. 220 nm – 260 nm.
3) Measurement of the temperature of the blackbody with the filter radiometer. If it had changed more than 0.2 %, steps 1-3 were repeated and the previous results discarded.
4) Measurement of the lamps with the SRIPS monochromator over the same wavelength range.
5) Measurement of the temperature of the blackbody with a filter radiometer
6) Measurement of the blackbody with the SRIPS monochromator over the same wavelength range
7) Measurement of the temperature of the blackbody with the filter radiometer.

In regions 3 and 4, the PMT detector suffered from short-term fatigue and long-term drift because of the higher signal levels. Therefore, the measurement sequence was altered:

1) Measurement of the temperature of the blackbody with a filter radiometer
2) Measurement of the blackbody with the SRIPS monochromator at one wavelength
3) Measurement of the lamp with the SRIPS monochromator at that wavelength
4) Measurement of the blackbody with the SRIPS monochromator at that wavelength
5) Repetition of steps 2 to 4 for all the other relevant wavelengths
6) Measurement of the temperature of the blackbody with the filter radiometer.

This process increased the time between measurements, and therefore allowed the PMT to recover between each light reading and also, by placing the blackbody and lamp measurements at one wavelength next to each other, reduced the effect of long-term drift.

4 Analysis of Measurement Results

4.1 Measurement Equation — Monochromator

At any wavelength, the SRIPS facility measures both the blackbody and the lamp. The signal when measuring the blackbody is:

$$V^{\mathrm{BB}}(\lambda) = \pi\, g \cdot \int R^{\mathrm{SRIPS,BB}}(l) \cdot L^{BB}(T,l) \cdot S(l,\lambda) \cdot dl + \text{stray light} + \text{electronic noise} \qquad (1)$$

Here, g is the geometric factor, which is described below. V^{BB} is the signal measured by the SRIPS detector, $R^{\mathrm{SRIPS,BB}}$ is the responsivity of the SRIPS facility during the blackbody measurements, L^{BB} is the radiance of the blackbody as given by Planck's law. S is the slit function of the monochromator, normalised to have a unit area and l is an integration constant, equivalent to wavelength, but only over the slit width. The integral is over the extent of the slit function, usually 5–10 nm. Over this wavelength range there will be a small change in the blackbody radiance and

also a (usually small) change in the SRIPS responsivity, therefore these functions lie inside the integral. Stray light and electrical noise are determined with a shutter.

The signal SRIPS measures when calibrating the lamp is given by a similar equation (A is the area of the integrating sphere aperture):

$$V^{\text{lamp}}(\lambda) = A \cdot \int R^{\text{SRIPS,lamp}}(l) \cdot E^{\text{lamp}}(\lambda) \cdot S(l,\lambda) \cdot dl + \text{stray light} + \text{electronic noise} \qquad (2)$$

When the second blackbody scan is made, the signal is given by Equation (1) again, although the stray-light and electrical noise may be different and the responsivity of SRIPS may have drifted a small amount. If the sources can be considered to be varying only slowly with wavelength over the slit function, then the integrals can be removed. This approximation is reasonable when the two sources are spectrally similar, as for a blackbody and FEL lamp. However, for dissimilar sources, an error is introduced, as is discussed in section 4.2.1. Taking this approximation, the two equations can be combined to give:

$$E^{\text{lamp}}(\lambda) = K\kappa(\lambda)\frac{\pi g}{A} L^{\text{BB}}(\lambda;T)\frac{V^{\text{lamp}}(\lambda)}{V^{\text{BB}}(\lambda)}\frac{R^{\text{SRIPS,BB}}(\lambda)}{R^{\text{SRIPS,lamp}}(\lambda)} \qquad (3)$$

Where E^{lamp} is the desired lamp irradiance. The final term should be unity, if the SRIPS facility has not drifted. It is left in at this stage for the purposes of uncertainty calculations. Here K is an additional constant introduced to account for any difference between the measured lamp geometry (alignment distance, tilt etc) and the defined lamp geometry at which the lamp should be measured. K is unity, but has an associated uncertainty.

In practice, the two measurements of the blackbody have been made at potentially different temperatures. The average of the two ratios: $L^{\text{BB}}/V^{\text{BB}}$ is used, where L^{BB} is calculated for the average of the blackbody temperature measured before and after the relevant monochromator scan.

The geometric factor comes from the form factor for radiative transfer between two coaxial circular discs, but is multiplied by the area of the emitting aperture in order to make a version that is symmetrical from one disc to the other:

$$g = \frac{2\pi r_1^2 r_2^2}{(r_1^2 + r_2^2 + d^2) + \sqrt{(r_1^2 + r_2^2 + d^2)^2 - 4r_1^2 r_2^2}} \qquad (4)$$

Here r_1 and r_2 are the radii of the two discs and d is the distance between them. For SRIPS measurements these are the radii of the blackbody and the integrating sphere aperture that is the entrance aperture to the monochromator system.

The radiance of a blackbody in air is calculated from Planck's law using air wavelengths and the refractive index of air, n.

$$L_{BB} = \frac{2h(c/n)^2}{\lambda^5(\exp[hc/n\lambda kT]-1)} \qquad (5)$$

4.2 Measurement Analysis

Due to the complicated nature of the measurements taken of the deuterium lamps, the measurement analysis occurs in several parts. Weighted shifts need to be applied to the data taken with the Spectralon tile diffuser since these measurements are considered only relative. Before the data was shifted the bandwidth of the monochromator and blackbody absorption were corrected for.

4.2.1 Bandwidth correction

Equation (3) makes the assumption that when Equation (2) is divided by (1) after the dark signal is removed, the responsivity of SRIPS cancels out. This would only be true if the slit function were infinitely narrow.

The question is how similar the measured ratio $\tilde{V}_{\text{lamp}}(\lambda)/\tilde{V}_{\text{BB}}(\lambda)$ is to the assumed ratio $V_{\text{lamp}}(\lambda)/V_{\text{BB}}(\lambda) = \dfrac{R(\lambda)E_{\text{lamp}}(\lambda)A}{R(\lambda)L_{\text{BB}}(\lambda)\pi g}$. The full integral equation is generally unsolvable. However, under certain specific conditions a solution can be found.

This problem has been investigated as part of a project [7] on lamp spectral modelling, and for a triangular slit function an approximation can be made. For a triangular slit function, of full width $2\Delta\lambda$ and a unit area, the following equation relating the assumed value to the measured value, and its second and subsequent derivatives, holds:

$$V(\lambda) = \tilde{V}(\lambda) - \tfrac{1}{12}(\Delta\lambda)^2\tilde{V}''(\lambda) + \tfrac{1}{240}(\Delta\lambda)^4\tilde{V}^{iv}(\lambda) + \ldots \qquad (6)$$

Equation (6) can be applied to each source and then the ratio taken. If the two sources are very similar (as is the case for an FEL calibrated against a blackbody), the correction to the ratio is tiny, even if the correction to each individual source is significant. This means that Equation (3) can be used without correction for FELs. However the blackbody and the deuterium lamps are very different sources and are changing rapidly and non-linearly in different directions, Figure 3. This means that Equation (3) can be used, but only after the raw signals (in V) are corrected for using Equation (6).

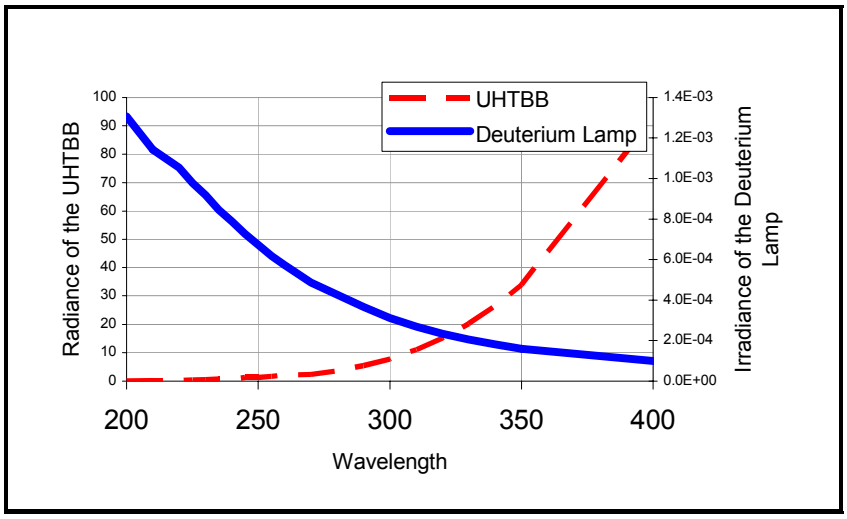

Figure 3 Radiance of the UHTBB and irradiance of a deuterium lamp

The correction that needs to be applied is the second term in Equation (6). The second derivative was calculated from the raw measurement data using the following equation:

$$V_i'' = \frac{d^2\tilde{V}_i}{d\lambda^2} = \frac{\tilde{V}_{i-1} - 2\tilde{V}_i + \tilde{V}_{i+1}}{d^2} \qquad (7)$$

Where *i* represent the discrete *i*th measurement and *d* is the step size between measurements. Therefore the correction is:

$$\Delta V = -\frac{(\Delta\lambda)^2}{12}\left[\frac{\tilde{V}_{i-1} - 2\tilde{V}_i + \tilde{V}_{i+1}}{d^2}\right] \quad (8)$$

This correction was applied to all of the lamp data before the weighted shifts were applied. In order to have measurements at appropriately spaced wavelengths to determine an accurate second derivative, measurements were made additionally on one day in each round in 2.5 nm steps. The correction calculated on that day was applied to all measurements on all days.

The bandwidth was determined by scanning a mercury line with the monochromator for the two slit widths used for the lamp measurements (slits of [3-3-5] corresponded to a bandwidth of 4.06 ± 0.05 nm, and slits [1-1-3] corresponded to a bandwidth of 1.46 ± 0.05 nm).

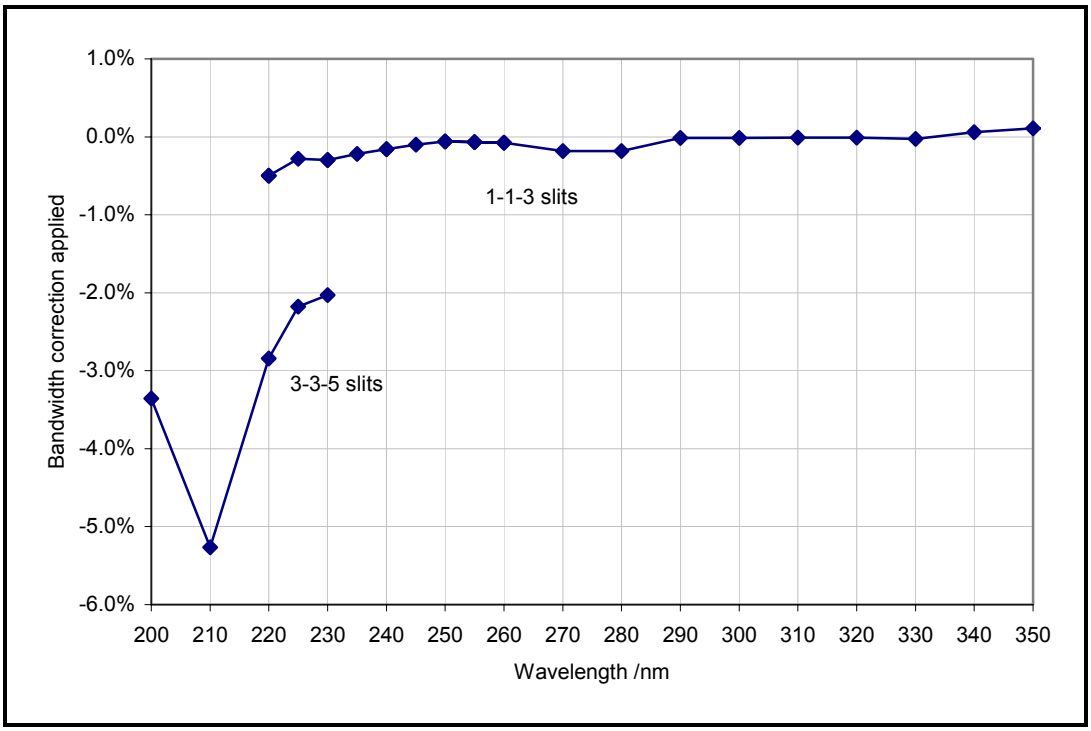

Figure 4 Bandwidth correction applied. Where there are two values for one wavelength it is because the monochromator is operated with different sized slits at those wavelengths. The stronger effect corresponds to the wider slits

4.2.2 Absorption correction

Investigations have shown [2] that the blackbody suffers from ultraviolet absorption around 380 nm. For this reason, the blackbody temperature was kept relatively low, around 3050 K for the longer wavelengths (regions 3 and 4).

To understand this and correct for this absorption effect, the blackbody was measured at different temperatures and the ratio of the measured signals between the hotter and cooler blackbodies was compared with the expected ratio from the Planck equation. A blackbody at 2450 K is assumed to show no absorption because there is no carbon sublimation, therefore a comparison of a blackbody at 3050 K with one at 2450 K, can be used to determine the absorption at the higher temperature. This showed a broad absorption feature in the region from 300 to 450 nm. The difference between these measurements was used as a correction in region 4.

These tests were also made at shorter wavelengths and for a hotter blackbody, since that was required for the shortest wavelengths to maximise signals there. It was not possible to make a

comparison to a blackbody cool enough to show no absorption; instead blackbodies at 3170 K and 3050 K were compared to one at 3000 K. Some absorption around 210 nm was discovered. The absorption is probably due to C_2N_2, which has strong lines at 209.31 nm and 210.74 nm [8].

The absorption correction for region 3 was based on the 3050 K blackbody results and the absorption correction for regions 2 and 1 were based on the 3170 K blackbody results. The overall absorption correction is plotted in Figure 5. The uncertainty in this correction is discussed in section 5.2.5.

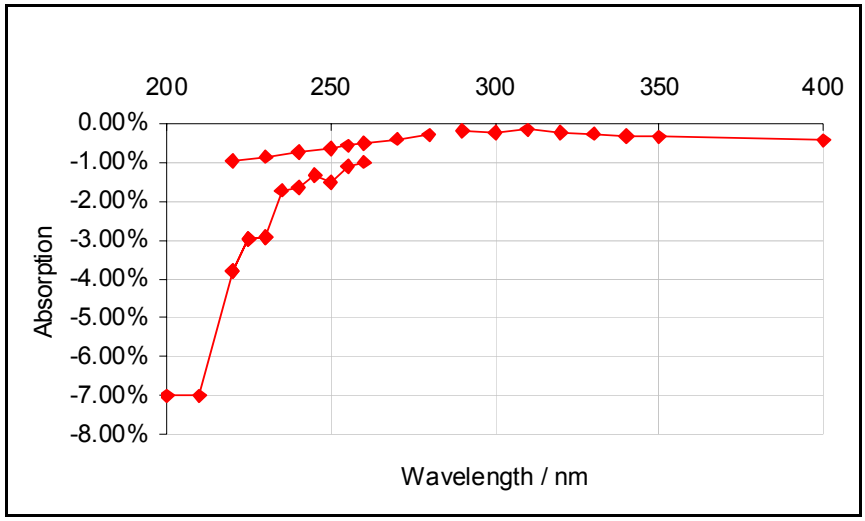

Figure 5 Absorption effect: Correction applied. Where there are two values for one wavelength, this is because the blackbody is operated at two temperatures at that wavelength. The stronger effect is seen at the higher temperature

4.2.3 Weighted Shift

The measurements made with the Spectralon tile diffuser at the lowest wavelengths are considered to be relative as they were made with no defining aperture. These measurements need to be shifted to agree with the measurements made with the integrating sphere. This shift was applied to the data after the absorption and bandwidth corrections had been applied.

Because the measurement was slightly different for regions 1 and 2, because of the slit size differences, region 1 requires two shifts, and region 2 requires one shift to be performed. Figure 6 shows an example of the simple calculation based on Equation (3) made for the lamp calibration on one day, (the example shown is from a comparison lamp).

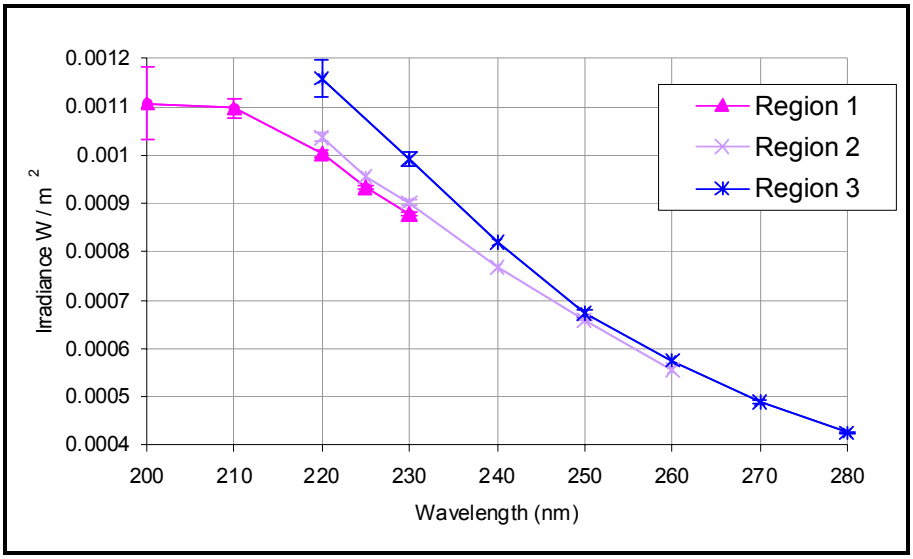

Figure 6 Raw calculation of deuterium irradiance, showing as "error bars" the blackbody repeatability during these measurements

In Figure 6 the "error bars" at each wavelength are different due to the repeatability of the blackbody. In region 3 the repeatability of the blackbody worsens at the lower wavelengths, this also occurs with the shortest lowest wavelengths in region 1. Since varying repeatability is highly wavelength dependent, the shifts that are applied are weighted according to their associated uncertainty. The uncertainty used for each wavelength was the standard deviation of the blackbody repeatability during the series of measurements, or the repeatability of the blackbody on the day of the measurement, which ever was the greater. This method was used so that any coincidently 'good' repeatability for an individual wavelength was averaged out so that an unbiased shift could be applied to the data.

The measurement made in region 1 [$A(\lambda)$], needs to be shifted by [α] and [β], to agree with the measurements made in region 3, [$A'(\lambda)$], Equation (9). Similarly the measurements made in region 2, [$B(\lambda)$], need to be shifted by [β] to agree with region 3, [$B'(\lambda)$]. α and β are the shift factors required, which were calculated by taking the weighted average of the overlapping wavelengths, Equation (10). ω_i is calculated using the repeatability of the blackbody, Equation (11).

$$A'(\lambda) = \alpha\beta A(\lambda) \qquad B'(\lambda) = \beta B(\lambda) \tag{9}$$

$$\beta = \frac{\sum_{i=1}^{N} \omega_i \left(\frac{C_i}{B_i}\right)}{\sum_{i=1}^{N} \omega_i} \tag{10}$$

$$\omega_i = \frac{1}{U\left(\frac{B_i}{C_i}\right)}, \text{ where } \quad U\left(\frac{B_i}{C_i}\right) = \sqrt{\left(\frac{U(B_i)}{B_i}\right)^2 + \left(\frac{U(C_i)}{C_i}\right)^2} \tag{11}$$

5 Uncertainty Analysis

5.1 Uncertainty in Constants

This section discusses the uncertainty in the constants in Equation (3) in section 4.1, K, g and A. K is a measure of the quality of the alignment of the lamp on the day of measurement. The lamps were aligned at a distance of 230 mm to the front of the glass envelope, and the uncertainty of that distance is estimated to be 0.3 mm. The lamp alignment uncertainty also contains estimates for the effect of minor tilt and similar alignment errors and has been estimated at 0.21 % for the deuterium lamps. Therefore K has a value of 1 ± 0.0021 for the scale lamps.

The lamp stability during the calibration was determined by monitoring the current of the deuterium lamp during the course of a measurement. This showed a standard deviation of 0.50 %. The stability from switch on to switch on was estimated by taking the standard deviation of the three scale lamp calibrations This gave an uncertainty of 1.50 %.

The uncertainty associated with an estimate of the value $\pi g / A$ is due to geometry. It is a constant at all wavelengths and for all separate lamp measurements. The effect is taken as a Type B uncertainty of 0.08 %. The relevant apertures are $r_1 = 4$ mm ± 0.1 μm, $r_2 = 8$ mm ± 0.1 μm and the distance between them is 500 mm ± 0.2 mm.

5.2 Uncertainty in Blackbody Radiance

The blackbody temperature is given by the Planck equation.

$$L^{BB}(\lambda;T) = \alpha(\lambda)\varepsilon \frac{2h(c/n)^2}{\lambda^5(\exp[hc/n\lambda kT]-1)} \tag{12}$$

Here h is the Planck constant, 6.626 0693(11) x 10^{-34} J s, c is the speed of light, 299 792 458 m s^{-1} (exact), k is the Boltzmann constant, 1.380 6505(24) x 10^{-23} J K^{-1} (CODATA 2002), n is the air refractive index, 1.00029 ± 0.00005 and ε is the emissivity of the blackbody, which is 0.99988 ± 0.00010, (see section 5.2.1.9).

$\alpha(\lambda)$ is from the absorption of the blackbody. A correction for this effect has been applied as shown in section 4.3.3. The associated uncertainty in the correction is discussed later in this section.

5.2.1 Uncertainty in blackbody temperature

The temperature of the blackbody is measured using a filter radiometer whose spectral responsivity, $R(\lambda)$, has been calibrated. The filter radiometer is placed in front of the blackbody and light is focussed onto it using a lens. Four measurements are taken: a light reading, V^{light}, a dark reading, V^{dark}, an out-of-band reading V^{OOB} (with a long-pass filter in front of the filter radiometer — this accounts for any filter radiometer responsivity at wavelengths longer than the longest calibration wavelength) and a dark out-of-band reading $V^{\text{OOB, Dark}}$, with the long pass filter and the shutter.

The signal, V, can be compared with the expected signal in the following equation:

$$\begin{aligned} V &= V^{\text{light}} - V^{\text{dark}} - V^{\text{OOB}} + V^{\text{OOB,Dark}} \\ &= sGUS \cdot g\pi R \cdot \int_{\lambda_0}^{\lambda_1} r(\lambda)\,\tau(\lambda)\,L(\lambda;T)\,d\lambda \end{aligned} \tag{13}$$

Here L is the radiance of the blackbody given by Equation (5), $\tau(\lambda)$ is the, wavelength-dependent lens transmittance, g is the geometric factor, given by Equation (4), but this time with the lens and filter radiometer apertures, G is the electronic gain of the amplifier and s is the size-of-source effect,

a measure of the amount of light scattered by imperfections in the lens. U is the uniformity of the blackbody—the difference between the signal measured and the signal that would be measured if a larger area of the blackbody were observed (because the spectral irradiance calibration facility sees a larger area of blackbody. S is a measure of the blackbody stability between the time when the temperature is measured and the time when the spectral irradiance is measured. S has a value of unity, but an associated uncertainty.

The responsivity of the filter radiometer has been split into two components. The absolute responsivity, R, (in A W^{-1}) has been separated from the relative spectral responsivity to simplify the error analysis (R is the component correlated at all wavelengths; r is entirely uncorrelated from one wavelength to the next).

The filter radiometer responsivity has been calibrated at discrete wavelengths; therefore, Equation (13) is replaced by a discrete version, using the trapezium rule:

$$V(T) = C\sum_{j=1}^{N} r_j L(\lambda_j, T)\cdot\delta\lambda_j \tag{14}$$

Here C combines all the uncertainties on the outside of the integral in Equation (13). $\delta\lambda_j$ is $\left(\lambda_{j+1}-\lambda_{j-1}\right)/2$ for all but the first $\left(\left(\lambda_2-\lambda_1\right)/2\right)$ and last $\left(\left(\lambda_N-\lambda_{N-1}\right)/2\right)$ values.

The Newton-Raphson technique is used to determine the temperature of the blackbody given the signal. This is robust for this calculation because only one value of temperature can be associated with each signal.

According to normal uncertainty analysis, as described in the Guide to the Uncertainty of Measurement (GUM) [9], given a function $f(x_1,x_2,x_3...)$, the uncertainty associated with the function, u_f should be derived from the uncertainties calculated from the individual parts. However, here the temperature cannot be described as a function of the other variables. Instead we must use the techniques for a "multivariate, implicit, real valued model" as described in section 6.3.4 of the 6th best practice guide from the Software Support for Metrology programme at NPL [10]. This requires Equation (14) to be written in the form $h(Y,X)=0$:

$$h(T,C,V,r_1...r_N,\tau_1...\tau_N) = \left[C\sum_{j=1}^{N} r_j L(\lambda_j,T)\cdot\delta\lambda_j\right] - V = 0 \tag{15}$$

The best practice guide supplies methods for determining the uncertainty in T due to the uncertainties in all the other components. The following equations are therefore needed to determine the uncertainty in temperature due to uncertainties in each of the components:

$$\left(\frac{\partial h}{\partial T}\right)^2 u^2(T) = u^2(V)\left(\frac{\partial h}{\partial V}\right)^2 + u^2(C)\left(\frac{\partial h}{\partial C}\right)^2 + \sum_{i=1}^{N} u^2(r_i)\left(\frac{\partial h}{\partial r_i}\right)^2 \tag{16}$$

$$\left(\frac{\partial h}{\partial T}\right)^2 = \left[C\sum_{j=1}^{N}\left(r_j\,\tau_j\,\delta\lambda_j\,\frac{\partial L(\lambda_j;T)}{\partial T}\right)\right]^2 \tag{17}$$

$$\left(\frac{\partial h}{\partial V}\right)^2 = 1 \tag{18}$$

$$\left(\frac{\partial h}{\partial C}\right)^2 = \left(\frac{V}{C}\right)^2 \tag{19}$$

$$\sum_{j=1}^{N}\left(\frac{\partial h}{\partial r_j}\right)^2 u^2(r_j) = \sum_{j=1}^{N}\left[C\,\tau_j\,L(\lambda_j;T)\delta\lambda_j\right]^2 u^2(r_j) \tag{20}$$

$$\frac{\partial L(\lambda_j;T)}{\partial T} = \frac{2h^2c^3\exp[hc/n\lambda kT]}{n^3\lambda^6 kT^2\left(\exp[hc/n\lambda kT]-1\right)^2} \tag{21}$$

These equations assume no correlation and there are no correlations between V and C (although there may be some correlations within C), nor between either of these and the r_j s. Since the blackbody was used at two different temperatures for the different regions for the measurement of the deuterium lamps, there are slightly different uncertainties that arise from the higher temperature and higher signal levels.

5.2.1.1 Uncertainty in signal levels

The signal level used in Equation (14) is the light signal level minus the dark signal and minus the out-of-band. This is treated as a type B uncertainty and comes dominantly from the uncertainty in the calibration of the voltmeter and the electrical noise in the dark reading. The uncertainty in the out-of-band comes from the quality of the filter used for the out-of-band measurements along with any differences between the temperature of the blackbody during out-of-band measurements and during blackbody temperature measurements.

The uncertainty in the measured signal is:

$$u_V^2 = u_{V^{\text{light}}}^2 + u_{V^{\text{dark}}}^2 + u_{V^{\text{OOB}}}^2 + u_{V^{\text{OOB, dark}}}^2 + \left(\frac{V}{K}\right)^2 u_K^2 \tag{22}$$

The final term represents the calibration uncertainty of the voltmeter. It assumes that it is the same for all four measurements and that they should all be multiplied by a, nominally unity, correction factor K. Therefore voltmeter non-linearities are assumed to be negligible. K is 1 with an uncertainty of 0.005 %.

Typically, V is 1.8 V and u_V is 0.09 mV. From Equations (18) and (16), this corresponds to a temperature uncertainty of 0.027 K.

5.2.1.2 Size-of-source

The size-of-source effect is 0.22 % ± 0.02 %, measured in accordance to the method described in [4]. From Equations (19) and (16), this corresponds to a temperature uncertainty of 0.10 K.

5.2.1.3 Amplifier gain

The amplifier was calibrated at an accredited laboratory. The quoted uncertainty on the amplifier measurements is 0.01 % at 95 % confidence, or a standard uncertainty of 0.005 %. From Equations (19) and (16), this corresponds to a temperature uncertainty of 0.03 K.

5.2.1.4 Lens transmittance

The lens transmittance was calculated using the Fresnel equations, which had previously [11] been shown to agree within 0.05 % of the measured value at this wavelength. From Equations (19) and (16), this corresponds to a temperature uncertainty of 0.15 K. Although the lens transmittance is a

wavelength dependent quantity and therefore inside the integral, the values are entirely correlated and therefore the uncertainty is considered in *C*.

5.2.1.5 Geometric factor

The geometric factor is derived from the size of the apertures on the filter radiometer and lens and the distance between them. However, the full expression for *g* is not required to work out the effect of these uncertainties. This is because the area of the filter radiometer aperture is used in calculating the spectral responsivity during its calibration, and this area is calculated from the same aperture calibration. This calculation is therefore exactly the same as that for the geometric factor in the spectral irradiance measurement. For a 0.1 μm uncertainty in the filter radiometer and lens aperture diameters and a 0.2 mm uncertainty in the distance, and for the normal set-up, *g/A* has a standard uncertainty of 0.07 %, which corresponds to a temperature uncertainty of 0.34 K.

5.2.1.6 FR absolute responsivity

The absolute responsivity of the filter radiometer after a fresh calibration has a standard uncertainty of 0.02 %. There is also an uncertainty due to any difference between the calibration set up of the filter radiometer and its use. The most significant problem with that is the size-of-source effect, which is large enough to be considered elsewhere, but the temperature of the filter radiometer and the f-number of the optical set-up are also important. Care is taken to make sure these conditions are matched as closely as possible. Therefore there is only a small additional uncertainty, of 0.01 % from this. An additional uncertainty of 0.04 % has been added to account for any filter radiometer drift. The overall uncertainty is 0.046 %, corresponding to a temperature uncertainty of 0.24 K.

5.2.1.7 Blackbody stability

When the blackbody is used as a reference source on the SRIPS facility, its temperature is measured twice before the monochromator scan and twice afterwards. If the difference between the maximum and minimum filter radiometer readings with an 800 nm filter radiometer is greater than 0.2 %, then the results are ignored and the scan repeated. The uncertainty in the averaged temperature is typically 0.05 %, corresponding to a temperature uncertainty of 0.26 K.

5.2.1.8 Blackbody uniformity

The uniformity of the blackbody is measured by scanning a filter radiometer with a 5 mm aperture in front of the blackbody at the distance of the integrating sphere. The central reading is similar to the temperature measurement and the overall scan is similar to the area of the integrating sphere aperture. The average of all the measurements is compared with the central reading. Of course a uniformity scan takes time and therefore the stability of the blackbody will also affect the measurement. However the stability is noisy at the 0.1 %-0.2 % level on a very short timescale. This means that there is no steady drift across the uniformity scan; instead, each individual point will have its own stability component completely uncorrelated with the points either side of it. This means that the averaging technique will also remove some of the stability uncertainty. The uncertainty in the uniformity correction is 0.11 %, corresponding to a temperature uncertainty of 0.33 K.

5.2.1.9 Emissivity

In addition to its effect in calculating the irradiance of the blackbody, the emissivity will also play a part in calculating its temperature. The emissivity of the BB3200pg blackbody was measured by colleagues in PTB [12] to be 0.999 7 ± 0.000 2. The emissivity of the BB3500 is assumed to be similar. Therefore the uncertainty in blackbody emissivity is 0.02 %, corresponding to a temperature uncertainty of 0.06 K. This does give a mathematical correlation between the blackbody irradiance calculation and temperature measurement but it is far too small to be significant.

5.2.2 Filter radiometer relative responsivity

The filter radiometer used was serial number 800W50S1337A (see section 2.5). The calibration of the filter radiometer has three distinct regions. In the wings, where the responsivity of the filter radiometer is low, the predominant uncertainty is signal to noise at around 0.5 % of the signal. On the steep slopes of the profile, the predominant uncertainty is due to wavelength fluctuations; this is expressed as a responsivity uncertainty of around 0.14 %. In the central, flatter region the signal to noise is good and any wavelength fluctuations are less significant. Here the uncertainty drops to 0.02 %. These uncertainties are entirely random and therefore the integration will average out their effect. The overall effect on temperature, calculated from Equations (22) and (25), is 0.005 K.

5.2.3 Uncertainty in trapezium rule

The numerical integration is carried out using the trapezium rule, because the filter radiometers have been calibrated at discrete wavelengths. An estimate of the uncertainty introduced by this can be obtained by calculating the temperature using all the points and then by using only half the points. The difference gives an uncertainty of 0.003 K at this temperature. Because of the large number of points (1150), this difference is small enough that more involved methods for determining the integral, and its uncertainty, are not required.

5.2.4 Overall uncertainty in temperature

Combining these equations and these uncertainty sources for a blackbody at 3050 K measured with filter radiometer 800W50S1337A, the overall standard (66 % confidence) uncertainty in temperature is 0.62 K. This value should be combined with the uncertainties of all the other components in Equation (12) to give the overall uncertainty in blackbody radiance. The effect of the temperature uncertainty on wavelength can be seen from that equation.

Uncertainty component	Uncertainty as a percentage of value, where appropriate		Temperature uncertainty/ K	
	3050 K	3160 K	3050 K	3160 K
Geometric factor	0.067 %	0.067 %	0.344	0.369
Blackbody Uniformity	0.064 %	0.064 %	0.328	0.351
Blackbody Stability	0.050 %	0.050 %	0.258	0.277
FR absolute responsivity	0.046 %	0.046 %	0.236	0.254
Lens Transmission	0.029 %	0.029 %	0.149	0.160
Size of source	0.020 %	0.020 %	0.103	0.110
Emissivity	0.012 %	0.012 %	0.060	0.064
Voltage measurement			0.027	0.031
Amplifier gain	0.005 %	0.005 %	0.026	0.028
FR relative responsivity			0.005	0.006
Mathematical Approximations			0.003	0.003
Overall Temperature Uncertainty			0.621 K	0.666 K

Table 3 Uncertainty components and overall uncertainty in the blackbody temperature measurement. All are standard uncertainties at the 66 % confidence level

5.2.5 Uncertainty in the absorption correction

Section 4.2.2, discusses the effect of absorption and the correction that has been applied to the data, since the absorption effect was significant. The ratios of the measurements at two different temperatures were compared to determine the absorption correction between 200 nm and 350 nm. The associated uncertainty in the correction is due to the uncertainty of the measurements made to determine the absorption effect, which is due to repeatability of those measurements. An

approximation was also made to account for the daily changes in the absorption. This daily effect was determined using some results from measurements made of the absorption on three separate dates. This variability was of the order of half to a third the correction factor; therefore the correction was divided by 2.5. These two uncertainties were added in quadrature.

The measurements in region 3 and 4 were performed at 3050 K and therefore absorption correction between 220 nm and 400 nm that was applied was from the measurements made at 3050 K. The uncertainties were determined in the same way, however the repeatability of these measurements and the correction applied was lower than for the shortest wavelengths, and therefore the uncertainties are lower.

5.2.6 Overall Uncertainty in blackbody radiance

The blackbody radiance is calculated from Equation (12). The uncertainty components to consider come from the temperature, as described in the previous section, the uncertainty in the correction of absorption due to carbon and, to a much smaller degree, to the uncertainty in the emissivity correction.

The overall standard uncertainty due to these factors is shown in Figure 7.

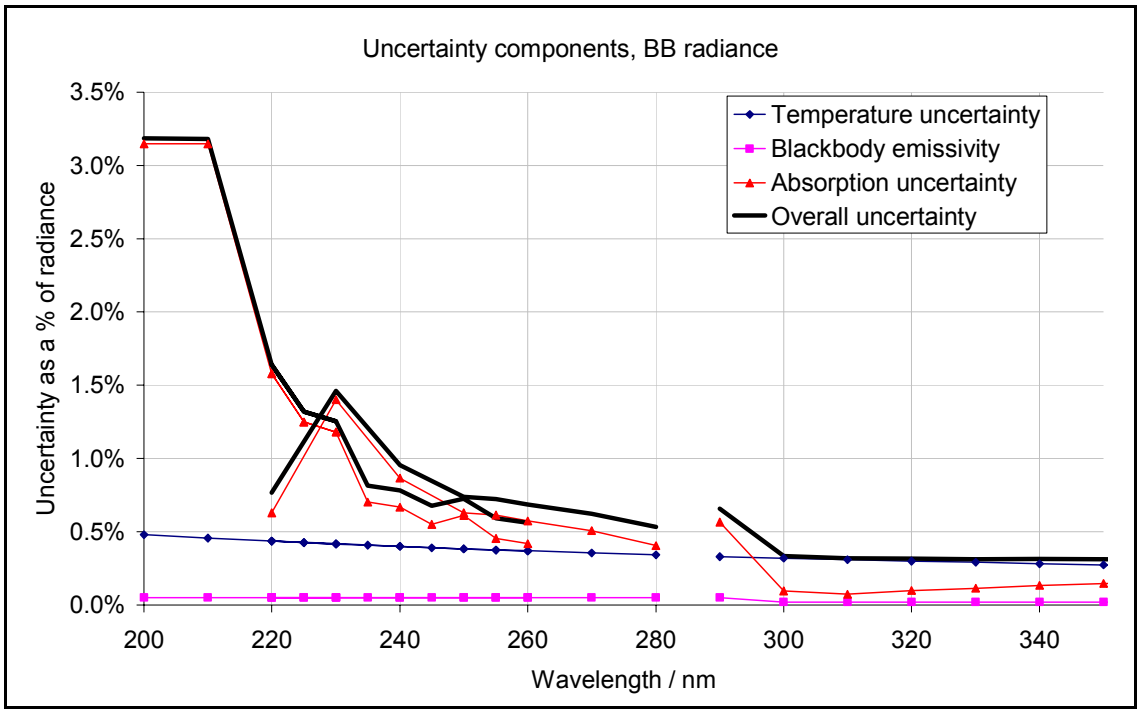

Figure 7: Standard uncertainty in blackbody radiance and a percentage of spectral radiance and as a function of wavelength

5.3 Uncertainty in Lamp-Blackbody Signal Ratios

The final uncertainty that needs to be considered is the uncertainty in the final two terms of Equation (3). That is the uncertainty in:

$$\frac{V^{\text{lamp}}(\lambda)}{V^{\text{BB}}(\lambda)}\frac{R^{\text{SRIPS,BB}}(\lambda)}{R^{\text{SRIPS,lamp}}(\lambda)} \tag{23}$$

The uncertainty in the ratios comes from any non-linearity in the response of the system or the measurement of the signals and in any drift in the facility between the measurement of the

blackbody and the measurement of the lamp, along with the noise on the signals. However there is an additional uncertainty due to whether this ratio is really the desired ratio, this uncertainty comes from the wavelength accuracy and the effect of the monochromator bandwidth.

5.3.1 Linearity

The uncertainty in V_{lamp}/V_{BB} is the uncertainty in the linearity [13] and repeatability of the voltage measurements with the voltmeter. Because of the ratio, the absolute calibration of the voltmeter is irrelevant. The linearity of the PMT is better than 0.1 % when the signal is below 1 μA.

5.3.2 Geometry match

When sources are compared to the blackbody they illuminate the defining aperture of the SRIPS facility (the integrating sphere aperture) slightly differently. To test the uncertainty associated with these differences, an FEL was measured in a variety of different geometries. The standard deviation of those measurements was 0.4 %. However that included lamp realignment. For these measurements the blackbody and deuterium lamp illuminate the sphere in a reasonably similar way, so 0.2 % is a reasonable estimate the residual effect.

5.3.3 Noise

The predominant uncertainty at most wavelengths is the uncertainty in the ratio $R_{SRIPS}^{BB}/R_{SRIPS}^{lamp}$.

The blackbody is measured before and after the lamp. The difference between these two measurements (when any change in temperature is accounted for) is due to the stability of the source and the stability of SRIPS. The source stability is insignificant because the source is highly stable, as measured by the filter radiometer; its insignificance is confirmed by the fact that the blackbody differences show no spectral component. Therefore it can be assumed that these differences give the repeatability of SRIPS. There is typically no drift from the first to the second blackbody scan. This means that the repeatability calculated between blackbody measurements is equivalent to the SRIPS repeatability between the blackbody and lamp measurements.

The differences have been measured on many occasions and variations from day to day are of statistical rather than of experimental significance. This uncertainty has been determined from a standard deviation of the differences between the blackbody measurements on measurements made during scale deuterium lamp calibration campaign. The results are shown in Figure 8.

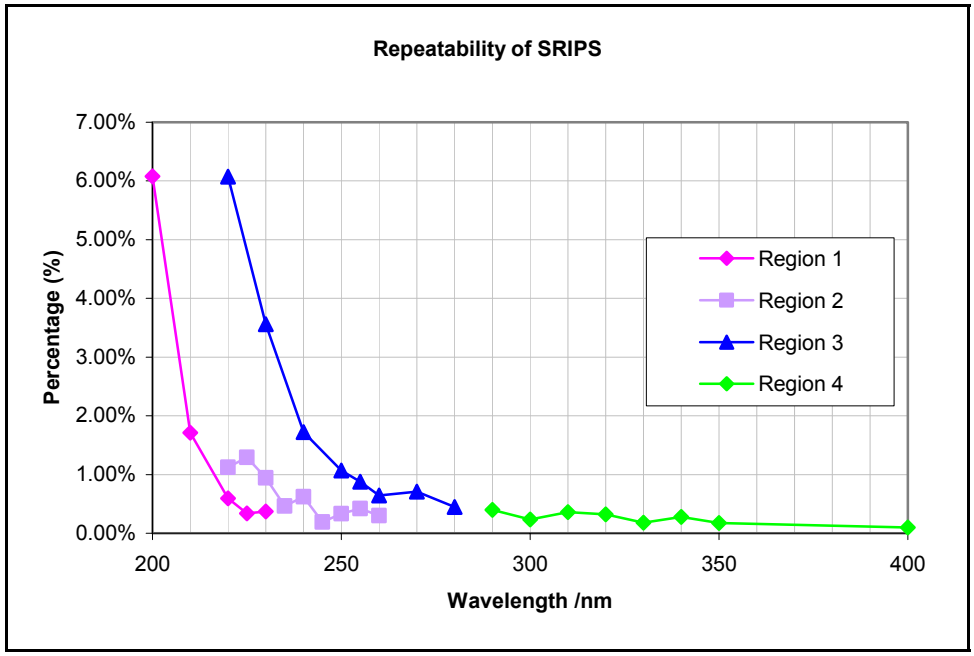

Figure 8 Repeatability of SRIPS.

The increases at the end of different spectral regions are due to the decrease in detector responsivity, a decrease in blackbody signal or a decrease in grating throughput which lead to a lower signal and higher noise. For FEL calibrations, the standard deviation of the two blackbody measurements has been considered as the uncertainty in the stability of the SRIPS facility. This is a reasonable assumption here too, for most of the spectral regions. However, for region 4, the blackbody signal is strong, while the deuterium lamp signal is extremely weak. Therefore in this region, the deuterium lamp signal is the dominant source of noise. For region 4, only, this repeatability has been multiplied by 2.

In practice when calculating the uncertainty on a particular day, the uncertainty is calculated either from this standard deviation of all days, or from the specific uncertainty on the day in question. This means that statistically good days are not advantaged, but that statistically poor days are disadvantaged.

5.4 Wavelength Accuracy

The ratios were carried out at the measured wavelengths, which may be slightly different to the calculated wavelengths because of uncertainty in the monochromator's wavelength accuracy. Strictly this should be treated as a wavelength uncertainty, however it can more easily be considered as an uncertainty in irradiance levels by looking at the effect of the wavelength error.

There is an uncertainty in the wavelength of around 0.05 nm. The effect of this depends on how smoothly varying both sources are, as well as how smooth the responsivity of SRIPS is. If the ratio of the signals of the two sources varies strongly with wavelength, the wavelength uncertainty will become more important. The Taylor expansion of V_{lamp}/V_{BB} is:

$$\tilde{V}(\lambda+\delta\lambda)=\frac{V^{\text{lamp}}(\lambda+\delta\lambda)}{V^{\text{BB}}(\lambda+\delta\lambda)}\approx\tilde{V}(\lambda)+\delta\lambda\cdot\frac{d\tilde{V}}{d\lambda} \qquad (24)$$

Therefore the uncertainties are calculated from the ratio of the second to the first term in Equation (24).

5.5 Uncertainty in the Bandwidth Correction

The bandwidth correction applied is that given in Section 4.2.1 and Equation (6). This discusses the uncertainty in that correction.

5.5.1 Uncertainty from the Measurement

This is the uncertainty due to the noise in the measurements on the day used to calculate the bandwidth correction. This noise is uncorrelated between the three points used to calculate the correction. Therefore the uncertainty due to the measurements can be obtained from:

$$u^2(\Delta V) = \left[\frac{\Delta\lambda^2}{12d^2}\right]^2 \left(u^2(V_{i-1}) + 4u^2(V_i) + u^2(V_{i+1})\right) + \left[\frac{2\Delta\lambda \cdot \left(V_{i-1} - 2V_i + V_{i+1}\right)}{12d^2}\right]^2 u^2(\Delta\lambda) \quad (25)$$

The uncertainty in the bandwidth, required for the second term in Equation (30), has been estimated as 0.05 nm. The uncertainty in each of the measurements is given by the standard deviation of the two measurements. Note that this is an *absolute* uncertainty, with units of V.

This has been used to calculate the uncertainty in the correction for both the blackbody measurement and for the lamp measurement. These are uncorrelated, so the uncertainty in the correction to the ratio of these can be obtained in the normal way by adding the two *relative* uncertainties in quadrature. The uncertainty calculated ranges from 1 % at 200 nm to 0.2 % for wavelengths above 220 nm.

5.5.2 Applicability to Other Days

To determine the bandwidth correction, measurements were required in very finely spaced intervals. This was only done on one day, so it is necessary to understand whether this correction can be applied to measurements of the other scale lamps on other days.

The effect due to the bandwidth being slightly different on another day is likely to be smaller than the 0.05 nm bandwidth uncertainty already considered in Equation (25).

The bandwidth correction was calculated for measurements made on a day when the blackbody was 100 K hotter. The difference was trivial compared to the uncertainties and can be neglected entirely for the 20 K variation from day-to-day during these measurements.

5.5.3 Different Lamps

The bandwidth correction was measured in detail only for the comparison lamp. However, on the 14 April 2004, preliminary bandwidth measurements were made* with both a scale lamp and a comparison lamp.

The difference between the corrections calculated for these methods is:

* These results aren't used, but the agreement between these and the 24 May 2004 results are for the comparison lamp excellent.

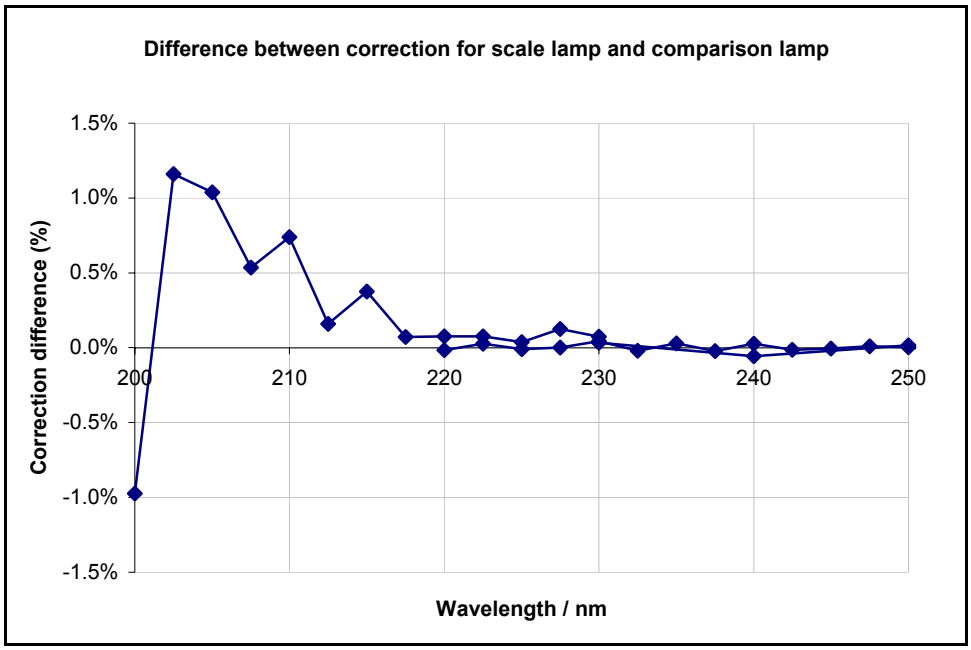

Figure 9 Difference between correction for scale lamp and comparison lamp

This difference is of the order of the repeatability uncertainty in the correction (Figure 9). Therefore for the use of this correction on comparison lamps, the uncertainty due to lamp variability is negligible, but for scale lamps, an additional term of this size was added to account for this difference.

5.5.4 Mathematical uncertainties

The mathematical uncertainty because of the approximation to a triangular slit function is not known, but these slit functions appear nominally triangular and we have already considered the uncertainty due to bandwidth errors. Therefore this uncertainty can be considered negligible.

The uncertainty due to stopping at the second derivative term can be found by calculating the fourth derivative term. The effect is completely negligible above 207.5 nm, but is of the order of 1.5 % for shorter wavelengths.

5.5.5 Overall uncertainty due to bandwidth correction

The overall uncertainty due to the bandwidth correction is given in Figure 10. The uncertainty in the correction is only significant at the shortest wavelengths where the monochromator is operated with wide slits and the original measurements were particularly noisy.

This uncertainty has been tested by comparing measurements made with the monochromator having different slit widths. The measurements disagreed before the bandwidth correction was applied, but after correction agreed within the appropriate uncertainties.

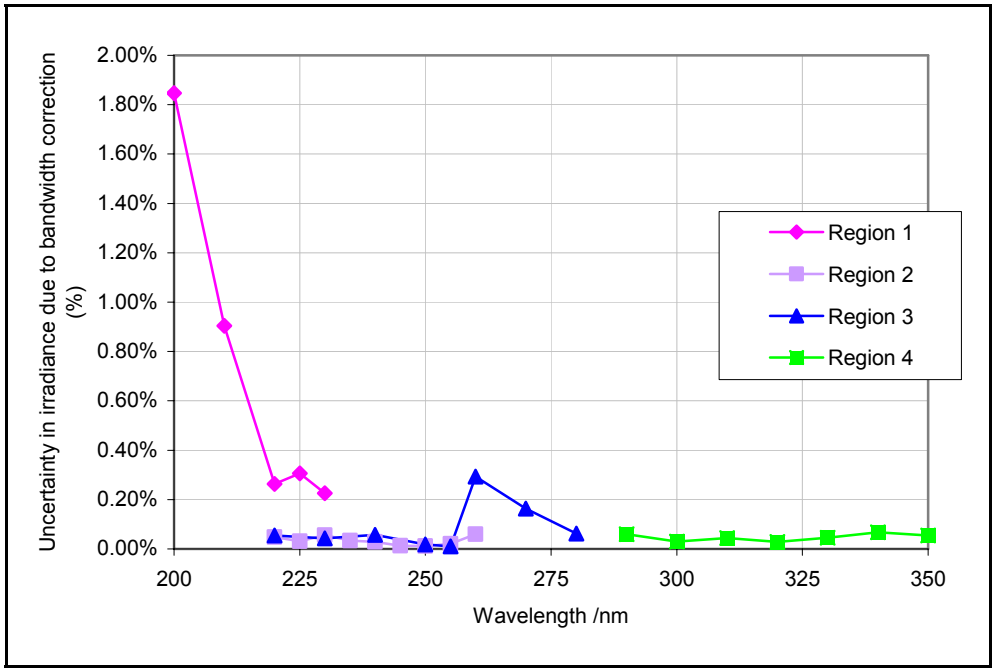

Figure 10 Uncertainty due to bandwidth correction (the correction itself is Figure 4)

5.6 Uncertainty in the Overlap Correction

The tile measurements in regions 1 and 2 (Table 2) must be corrected to overlap with the sphere measurements in regions 3 and 4. This is performed using the equations in section 4.2.1. Because this overlap is made, the systematic uncertainty in regions 1 and 2, due, for example to detector linearity, will not matter, except that because it is the same uncertainty in region 3 it will be reintroduced as the systematic component of the correction uncertainty*.

In addition to this systematic uncertainty, there is a random component to the uncertainty. If the raw measurements are very noisy, then the correction will be less accurate. However, if some points are noisier than others, then the weight will have reduced their effect anyway. So, this has to be calculated to account for both these effects.

The uncertainty used was based on the comparison lamp DLS-NPL-L#01 and the measurements of it during the first round. Using the same notation as in section 4.2.1, the uncertainty due to noise in β can be calculated from:

$$u^2(\beta) = \sum \left[\left(\frac{C_i}{B_i} - \beta \right) \omega_i \right]^2 \qquad (26)$$

The uncertainty in α is similar, but the uncertainty in the A to C correction must add the β and α uncertainties in quadrature. This was done for the three calibrations of the comparison lamp DLS-NPL-L#01 in the first round and from these an overall uncertainty of 2.01 % for the region 1 to region 3 correction and 1.94 % for the region 2 to region 3 correction was deduced and applied to all calibrations of all lamps. The comparison lamps were similar enough to the scale lamps for the same uncertainties to be applied here.

* Of course if the systematic component was different in region 3 from region 2 it would be the region 3 uncertainties that would matter here.

6 Overall Uncertainty in Lamp Irradiance

6.1 Single Lamp Calibration

The standard uncertainty (66 % confidence) for a single calibration of a lamp can be obtained by combining in quadrature the uncertainties discussed in section 5. This is shown in Figure 11. This figure includes lines for each region, as listed in Table *2*, which is why there is more than one value for some wavelengths. The final lamp results were calculated by combining the measurements from different regions using a weighted average. Because the average is weighted, the uncertainty will approach that of the lower uncertainty measurement at each wavelength. These are the uncertainties for a single measurement of a scale lamp, they are partially reduced when, for example, three measurements are averaged. The uncertainties are also lower for more stable lamps, for example the lamps used for the CCPR K1.b Key Comparison. The uncertainty for a single measurement of those lamps (also reducible through averaging) is shown in Figure 12.

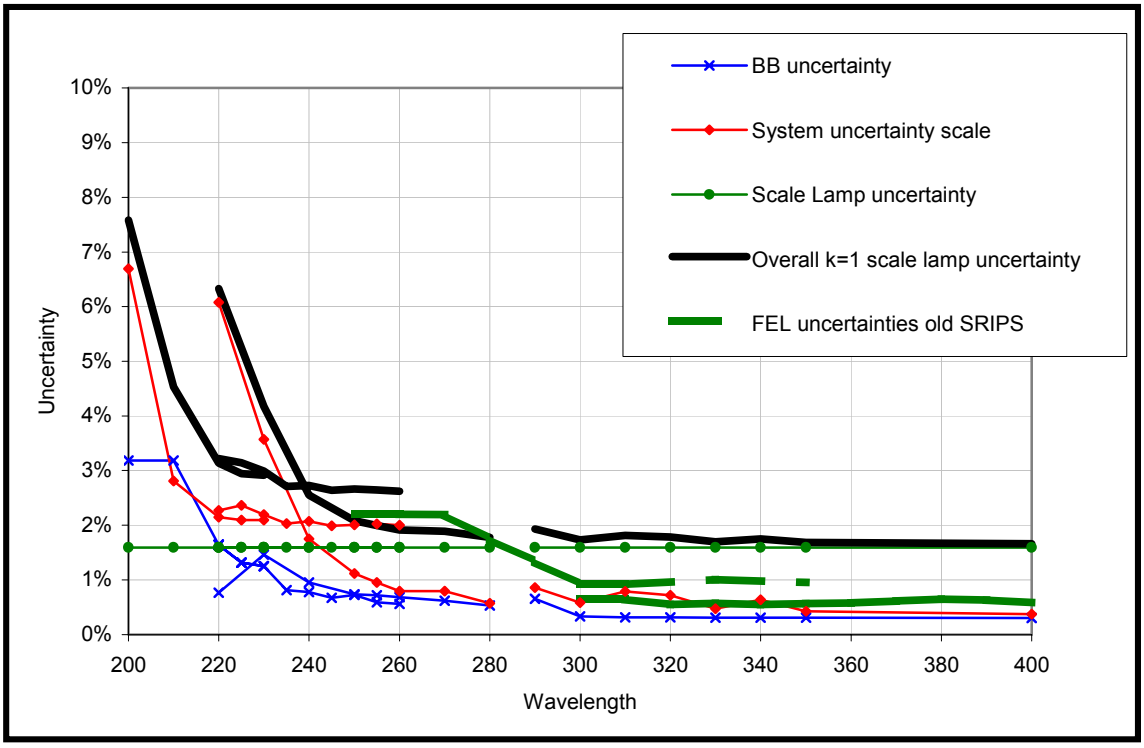

Figure 11 Overall k=1 uncertainty for a single measurement of a scale deuterium lamp

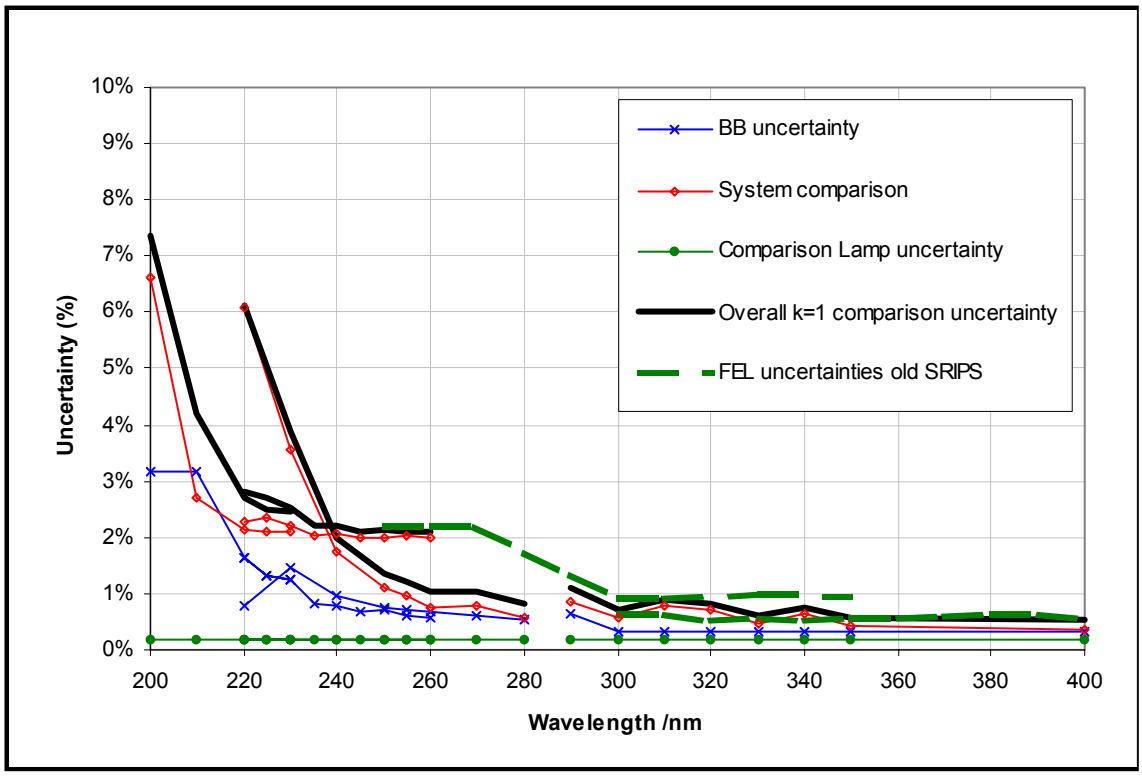

Figure 12 Overall k=1 uncertainty for a single measurement of a comparison deuterium lamp

6.2 Multiple Calibrations of a Lamp

The three calibrations of the lamp were combined using a simple average. The uncertainty on this average will be better than the uncertainty of the individual calibration because of the process of averaging. However this improvement will only affect the uncertainties associated with effects that are uncorrelated from one measurement to the next. These uncertainties can be reduced by $\sqrt{3}$, but the correlated uncertainties will remain unchanged.

Correlated Effects	Uncorrelated Effects
Blackbody temperature	Measurement noise/repeatability
Blackbody emissivity	Overlap random effects
Original measurement of blackbody absorption	Day-to-day variability of blackbody absorption
Linearity	Lamp alignment
Geometry mismatch	Lamp daily stability
Bandwidth	Lamp stability between switch-ons
Wavelength error	
Systematic overlap correction	

Table 4 Uncertainty components split between correlated and uncorrelated

6.3 Increased Uncertainty in 270 to 310 nm region

These measurements were made at the same time as the CCPR K1-b comparison measurements. As part of this comparison, the lamps were measured by NPL on two occasions. In most regions the repeatability of the lamps was exactly as statistically expected due to the calibration uncertainties.

However, unfortunately in the 270 to 310 nm region, the repeatability was noticeably larger than the uncertainty.

A series of investigations carried out failed to identify a clear cause of this change. However, the results for the second round measurements are spectrally “smoother” and more realistic. It is therefore assumed that there was an unidentified error causing this discrepancy during the first round measurements. It is unfortunate that it has not been possible to reproduce and understand this error. The scale lamps were recalibrated on one occasion in this region only. The results of that single measurement were scaled to make the 260, 320 and 330 nm points overlap with the average of the previous three calibrations.

The uncertainty was increased because these points were based on one measurement rather than three, and again by a factor of half the change seen between the first and second rounds of the comparison measurements.

6.4 Overall Uncertainties

The uncertainties have originally been calculated for one measurement of the lamp in each region independently. These uncertainties are shown in Table 5. Those uncertainties highlighted are reduced by $\sqrt{3}$ when combining three measurements of the lamp – in the problem region only one measurement is used and therefore the uncertainties are not reduced. Certain components within the blackbody radiance can also be reduced.

Wavelength	Blackbody radiance	Linearity of system	Geometry match	Bandwidth	Wavelength accuracy	Noise	Overlap systematic	Overlap random	Lamp alignment	Lamp stability during day	Lamp stability from on to on	270 - 310 nm extra measurement 1
200	3.19 %			1.57 %	0.62 %	6.08 %	0.22 %	2.01 %	0.21 %	0.50 %	1.50 %	
210	3.18 %			0.52 %	0.21 %	1.71 %	0.22 %	2.01 %	0.21 %	0.50 %	1.50 %	
220	1.64 %			0.25 %	0.29 %	0.60 %	0.22 %	2.01 %	0.21 %	0.50 %	1.50 %	
225	1.32 %			0.30 %	0.30 %	0.34 %	0.22 %	2.01 %	0.21 %	0.50 %	1.50 %	
230	1.26 %			0.03 %	0.33 %	0.94 %	0.22 %	1.94 %	0.21 %	0.50 %	1.50 %	
235	0.82 %			0.02 %	0.30 %	0.46 %	0.22 %	1.94 %	0.21 %	0.50 %	1.50 %	
240	0.78 %			0.01 %	0.30 %	0.62 %	0.22 %	1.94 %	0.21 %	0.50 %	1.50 %	
245	0.68 %			0.01 %	0.31 %	0.19 %	0.22 %	1.94 %	0.21 %	0.50 %	1.50 %	
250	0.74 %	0.10 %	0.20 %	0.00 %	0.23 %	1.07 %			0.21 %	0.50 %	1.50 %	
255	0.73 %	0.10 %	0.20 %	0.01 %	0.31 %	0.88 %			0.21 %	0.50 %	1.50 %	
260	0.69 %	0.10 %	0.20 %	0.05 %	0.28 %	0.64 %			0.21 %	0.50 %	1.50 %	
270	0.63 %	0.10 %	0.20 %	0.05 %	0.24 %	0.71 %			0.21 %	0.50 %	1.50 %	0.5 %
280	0.54 %	0.10 %	0.20 %	0.05 %	0.27 %	0.45 %			0.21 %	0.50 %	1.50 %	0.75 %
290	0.66 %	0.10 %	0.20 %	0.06 %	0.25 %	0.79 %			0.21 %	0.50 %	1.50 %	1.25 %
300	0.34 %	0.10 %	0.20 %	0.03 %	0.27 %	0.47 %			0.21 %	0.50 %	1.50 %	0.75 %
310	0.33 %	0.10 %	0.20 %	0.04 %	0.25 %	0.72 %			0.21 %	0.50 %	1.50 %	0.50 %
320	0.33 %	0.10 %	0.20 %	0.03 %	0.24 %	0.64 %			0.21 %	0.50 %	1.50 %	
330	0.32 %	0.10 %	0.20 %	0.04 %	0.21 %	0.36 %			0.21 %	0.50 %	1.50 %	
340	0.32 %	0.10 %	0.20 %	0.07 %	0.21 %	0.55 %			0.21 %	0.50 %	1.50 %	
350	0.32 %	0.10 %	0.20 %	0.05 %	0.08 %	0.35 %			0.21 %	0.50 %	1.50 %	
400	0.31 %	0.10 %	0.20 %	0.10 %	0.20 %	0.20 %			0.21 %	0.50 %	1.50 %	

Table 5 Overall uncertainty components that make up the uncertainties. "Blackbody radiance" includes blackbody temperature (see Table 3), blackbody absorption, blackbody emissivity and blackbody – integrating sphere geometry. All uncertainties are standard uncertainties, k=1.

The overall standard uncertainties for the scale lamps calibrated in April 2004, have been split into those fully correlated between measurements of different lamps. This combines three calibrations. This combination is shown in Table 6.

Wavelength	Fully correlated	Fully uncorrelated	Overall *k*=1	Overall *k*=2
200	2.48 %	4.14 %	4.83 %	9.65 %
210	1.79 %	2.40 %	3.00 %	5.99 %
220	0.77 %	1.76 %	1.92 %	3.83 %
225	0.74 %	1.65 %	1.81 %	3.61 %
230	0.60 %	1.69 %	1.79 %	3.59 %
235	0.57 %	1.53 %	1.63 %	3.26 %
240	0.56 %	1.54 %	1.64 %	3.28 %
245	0.56 %	1.49 %	1.59 %	3.18 %
250	0.76 %	1.12 %	1.36 %	2.71 %
255	0.78 %	1.06 %	1.32 %	2.63 %
260	0.80 %	1.73 %	1.91 %	3.82 %
270	0.86 %	1.75 %	1.95 %	3.91 %
280	0.98 %	1.66 %	1.93 %	3.86 %
290	1.45 %	1.78 %	2.30 %	4.60 %
300	0.89 %	1.66 %	1.89 %	3.77 %
310	0.68 %	1.75 %	1.88 %	3.76 %
320	0.45 %	1.72 %	1.78 %	3.56 %
330	0.43 %	0.95 %	1.04 %	2.08 %
340	0.42 %	0.98 %	1.07 %	2.13 %
350	0.37 %	0.95 %	1.02 %	2.03 %
400	0.40 %	0.93 %	1.02 %	2.03 %

Table 6 Uncertainties combined for three measurements of the lamp

7 References

[1] N. P. Fox, Primary radiometric quantities and units, *Metrologia*, **37**, 507-513, 2000

[2] E. R. Woolliams, N. J. Harrison, B.B. Khlevnoy, L.J. Rogers, N.P. Fox, Realisation and dissemination of spectral irradiance at NPL. *UV News*, 7, **pp 39-42,** 2002

[3] P. Sperfeld, S. Galal Yousef, J. Metzdorf, B. Nawo, W. Möller, The use of self-consistent calibrations to recover absorption bands in the black-body spectrum. *Metrologia*, **37(5),** pp. 373-376, 2000

[4] Fox N.P., Martin J.E., Nettleton D.H., "Absolute spectral radiometric determination of the thermodynamic temperatures of the melting/freezing points of gold, silver and aluminium", *Metrologia*, **28**, pp 357-374, 1991

[5] E.R. Woolliams, D.F. Pollard, N.J. Harrison, E. Theocharous and N.P. Fox, New facility for the high-accuracy measurement of lens transmission. *Metrologia*, **37(5),** pp 603-605, 2000

[6] Valerie E. Anderson, Nigel P. Fox, David H. Nettleton, Highly stable, monochromatic and tunable optical radiation source and its application to high accuracy spectrophotometry, *Applied Optics*, **31(4)**, pp 536-545, 1992

[7] Cox M.G., Harris P.M., Kenward P.D., Woolliams E.R., "Spectral characteristic modelling", *NPL Report CMSC* **27/03**. Available at: http://www.npl.co.uk/ssfm/download/

[8]R.W.B Pearse and A.G.Gaydon, *The identification of molecular Spectra. Third Edition*, Chapman and Hall Ltd. 1965

[9] Guide to the Expression of Uncertainty in Measurement, Geneva, International Organization for Standardization, 1993

[10] M. G Cox, PM Dainton, PM Harris, Software Support for Metrology, Best Practice Guide No. 6: Uncertainty and statistical modelling", March 2001, available at: http://www.npl.co.uk/ssfm/download/

[11] E.R. Woolliams, D.F. Pollard, N.J. Harrison, E. Theocharous and N.P. Fox, New facility for the high-accuracy measurement of lens transmission. *Metrologia*, **37(5)**, pp 603-605, 2000

[12] S. Galal-Yousef, P. Sperfeld, J. Metzdorf, "Measurement and calculation of the emissivity of a high-temperature blackbody", *Metrologia*, **37(5)**, 365-368, 2000

[13] E. Theocharous, J. Ishii, N. p. Fox, Absolute linearity measurements on HgCdTe detectors in the infrared region, *Applied Optics*, **Vol 43, No.21**, 2004